The two-year radiometric evaluation of Sentinel-3A OLCI via intersensor comparison with SNPP VIIRS

Mike Chu and Menghua Wang

***Abstract*— The on-orbit calibration performance of the Ocean and Land Colour Instrument (OLCI) onboard the Sentinel-3A satellite, launched on 16 February 2016, is evaluated via a radiometric intersensor comparison referencing to the Visible Infrared Imaging Radiometer Suite (VIIRS) onboard the Suomi National Polar-orbiting Partnership (SNPP) satellite. Among the 21 OLCI bands (designated as "Oa" bands), which are reflective solar bands (RSBs), seven of the OLCI bands match up sufficiently well with the seven shortest wavelength SNPP VIIRS bands (M1 to M7) – they are Oa02 at 412.5 nm, Oa03 at 442.5 nm, Oa04 at 490 nm, Oa06 at 560 nm, Oa08 at 665 nm, Oa12 at 754 nm and Oa17 at 865 nm. The radiometric comparison adopts a "nadir-only" refinement of the simultaneous nadir overpass (SNO) approach and uses the official SNPP VIIRS RSB data processed by the Interface Data Processing System (IDPS). The time series result for bands Oa02, Oa03, Oa08 and Oa17, with spectral coverage well represents the spectral range of OLCI, shows two-year stability at the level of 0.3% that supports nominally correct on-orbit calibration. The result for Oa08, Oa09 and Oa10, the three spectrally adjacent bands matching to M5, demonstrates the effects of spectral mismatch — different radiometric ratio baselines and seasonally modulating patterns. Lastly, this result clarifies some key findings from earlier studies involving SNPP VIIRS, and illustrates great potential for significantly more radiometric evaluation activities in the new era of Earth observations with many more powerful multispectral sensors coming into operation.**

***Index Terms*— VIIRS, OLCI, RSB, Reflective solar bands, SNPP, Sentinel-3A, Inter-sensor comparison, Intercalibration, On-orbit calibration, SNO.**

I. Introduction

The launch of the Ocean and Land Colour Instrument (OLCI), and its companion instrument the Sea and Land Surface Temperature Radiometer (SLSTR) [1,2], by the European Space Agency (ESA) on 16 February 2016 aboard the Sentinel-3A satellite takes one more progressive step for the observation of Earth environment by high-performing polar-orbiting multispectral instruments. The main objective of the Sentinel-3A mission is to measure sea surface topography, land and sea surface temperature, and land and ocean surface color for ocean forecasting, environmental monitoring and climate monitoring. OLCI is a main instrument in Sentinel-3A comprising 21 reflective solar bands (RSBs) dedicated to the ocean color (OC) applications, covering the spectral range from 0.4 to 1.02 μm, from the visible (VIS) to the near-infrared (NIR) range.

For evaluating the post-launch radiometric performance of Sentinel-3A OLCI, specifically of its on-orbit calibration performance, this study carries out a radiometric intersensor comparison referencing to the Visible Infrared Imaging Radiometer Suite (VIIRS) housed in the Suomi National Polar-orbiting Partnership (SNPP) satellite that was launched on 28 October 2011 [3]. SNPP VIIRS has 11 moderate-resolution RSBs (with 750 m spatial resolution), with 7 of the RSBs within the OCLI spectral coverage under 1020 nm and can be well matched to 7 corresponding OLCI bands. While SNPP VIIRS also contain imaging bands (at 375 m spatial resolution), this study does not utilize its imaging bands since moderate-resolution bands are sufficient for this study. The comparison methodology utilizes the simultaneous nadir overpasses (SNOs) [4−6] of the two satellites to compare the respective radiances over the concurrently observed Earth scenes. Specifically, a radiometric intersensor comparison assesses the performance of the post-launch on-orbit calibration, and any features deviating away from a stable time series signal some inaccurate on-orbit calibration in either of two sensors. Thus, this study necessarily relies on SNPP VIIRS being a reasonably reliable radiometric reference. The successful comparison will be important for OC products activities and can place OLCI products on par with those of SNPP VIIRS.

It is important here to note that the RSB calibration of SNPP VIIRS has been rigorously examined [7-13]. The current official release of the sensor data records (SDR) set [14], generated by the Interface Data Processing Segment (IDPS), is known to contain inaccuracy and instability [7-10,15,16], including an inherent calibration error causing worsening long-term drift [8-10,17]. An inter-RSB comparison studies by Chu et al. [18-20] using a "nadir-only" approach have also examined the radiometric performance of the IDPS version of SNPP VIIRS SDR and also an independently calibrated version generated by the NOAA OC team by utilizing the MODerate-resolution Imaging Spectroradiometer (MODIS) on the Aqua satellite as a reference. It was demonstrated that the IDPS SDR drifts radiometrically up to about 0.3% per year in particular for M1 to M4, the four bands of the shortest wavelength. This level of deviation in IDPS SDR is not expected to be statistically significant for this two-year study and that the use of the IDPS version of SNPP VIIRS radiometric data is sufficient for comparing with OLCI data. In addition, the short-wavelength RSBs of MODIS have also been shown to have radiometric drift [17]. It is possible that OLCI, with a similar

This paper is submitted on May XX, 2019.

M. Chu is with the NOAA Center for Satellite Applications and Research, College Park, Maryland 20740 and Cooperative Institute for Research in the Atmosphere, Colorado State University, Fort Collins, CO 80521 USA (e-mail: mike.chu@noaa.gov).

Menghua Wang is with the NOAA Center for Satellite Applications and Research, College Park, Maryland 20740 (e-mail: menghua.wang@noaa.gov).

on-orbit calibration strategy and components, also contains radiometric drift in its short-wavelength bands.

For the SNO analysis for detecting the aforementioned radiometric drift and other deviations, this study adopts the "nadir-only" refinement that has been successfully applied for SNPP VIIRS versus Aqua MODIS [18-20]. The "nadir-only" adaptation uses a small area centered at nadir-crossing to approximate the small viewing angle condition to eliminate confounding issues arising from larger areas or viewing angles, including the systematic response-versus-scan angle (RVS) effect and the more general angle-dependent effect of bidirectional reflectance distribution function (BRDF). This study therefore continues on with the "nadir-only" approach for assessing the on-orbit RSB calibration performance of OLCI that avoids the various confounding effects associated with larger areas. Thus, this study demonstrates the general applicability of the "nadir-only" methodology to inter-RSB comparison of multispectral sensors.

This paper is organized as follows. Section II briefly presents the instruments. Section III provides a short description of analysis and procedure. Section IV presents the comparison result. Section V presents a brief discussion. Section VI concludes and provides a summary.

II. The Instruments

Table 1 lists some key orbit parameters of Sentinel-3A and SNPP satellites, along with some sensor specifications for Sentinel-3A OLCI and SNPP VIIRS.

All 21 Sentinel-3A OCLI bands are RSBs operating below 1020 nm in wavelength that follow a regular on-orbit calibration operation schedule. Table 2 lists the matching Sentinel-3A OLCI and SNPP VIIRS bands. The designation for OLCI bands is Oa01, Oa02, and so on, up to Oa21. The spectrally matching SNPP VIIRS bands to Sentinel-3A OLCI are the moderate-resolution bands (M-bands) M1−M7, at 750 m resolution, and imagery bands (I-bands) I1 and I2, at 375 m resolution. This analysis uses only the M-bands of SNPP VIIRS for comparison analysis. There are seven band-pairs for inter-RSB comparison, as shown in Table 2, not including Bands I1 and I2 of SNPP VIIRS.

For convenience and for the remainder of the paper, the band designation will be stated without referencing to the satellite and the sensor, such as "Oa2 versus M1", without ambiguity.

III. Procedure and Analysis

The "nadir-only" refinement of the SNO analysis for inter-sensor comparison was first tested in an examination of SNPP VIIRS versus Aqua MODIS [19]. A brief description of this adopted analysis for Sentinel-3A OLCI versus SNPP VIIRS in the "nadir-only" framework is provided here. The "nadir-only" adaptation restricts the radiometric comparison to a small area centered at the nadir-crossing of each SNO occurrence to approximate the small viewing angle condition in order to eliminate confounding issues arising from larger areas or viewing angles, including the systematic RVS effect, such as known for MODIS [21,22], and the more general angle-dependent effects including the BRDF. For this analysis, the size of the comparison area has been examined and selected to be 32×32 km-square, for which the viewing angle is under 2.5°. The Sentinel-3A data are publically available starting October 2016 [23], and data up to January 2019 are used for this analysis.

A. SNO Occurrences

Close to 2000 SNO events, with time difference under 15 minutes, are found between October 2016 and January 2018. The location of the nadir crossing is precisely determined within a single pixel - all SNOs occur within a narrow circular band at around 71.0°N latitude. For demonstration, Fig. 1 shows the subset of SNOs that generated successful comparisons.

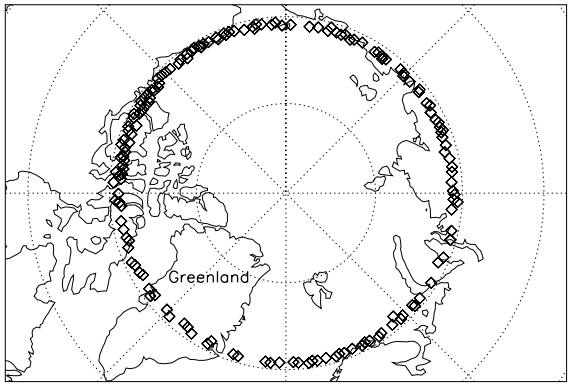

Figure 1: The SNOs of Sentinel-3A OLCI versus SNPP VIIRS occur exclusively in the northern polar region within a narrow band around 71°N latitude.

The search for SNOs, surprisingly, found two extended four-month gaps in each of the two years of the Sentinel-3A operation. It has been determined that because OLCI observational coverage changes over the course of the year, OLCI coverage higher than 71°N latitude becomes missing during this period. It is presumed that the missing data recur yearly and that some missing SNOs results will be true for Sentinel-3A OLCI regardless of which other sensor is used. These four-month gaps will also appear in the comparison time series shown later.

B. Comparison Area Size, Sampling Procedure and the Time Series

The study uses a homogeneity-ranked, sample-size constrained procedure to carry out sampling analysis of radiometric comparison within each SNO event. A small area, close to 32×32 square-km, centered at the nadir crossing of each SNO event is used for sampling analysis. Specifically, a size of 108×108 pixels (32.4 km) is used for OLCI and 44×44 pixels (33.0 km) is used for VIIRS. Because OLCI pixels are of smaller size at 300 m, each VIIRS pixel at 750 m overlaps numerous OLCI pixels. The one OLCI pixel whose center is closest to the center of the VIIRS pixel, using geolocation information of each pixel, is selected to be the unique matching collocated pixel. As it is each VIIRS pixel that is being matched to a unique collocated OLCI pixel, this inter-sensor comparison analysis operates at the 750 m regime.

A pixel-based radiometric ratio is computed for each pair of matching pixels of the SNO event by taking the OLCI radiance over the VIIRS radiance:

$$r = \frac{RAD_{OLCI}}{RAD_{VIIRS}}$$

This builds up a two-dimensional array of ratio the size of 44×44 pixels, or a total of 1936 pixel-based ratios per SNO event. It is noted that a smaller area, such as a 20×20 square-km size for maximally 900 pixel-based ratios, can be used for a more constrained comparison but at the cost of reducing the number of available pixels. Various area sizes have been tested. The 32×32 square-km is a reasonable balance between generating enough number of pixel-pairs and avoiding too large area or angle.

C. Pixel-based Homogeneity

Each pixel-based ratio is evaluated for its homogeneity, represented by the percentage standard deviation (STD) calculated using the pixel and its eight neighbors. This criterion is used to remove pixel regions with greater variability. The threshold for homogeneity is set at 4.5%, and any pixel-based ratios greater than the set threshold are excluded. It is here noted that the choice of 4.5% is not stringent but simply a choice that works.

D. Sample Size

The sample size of pixels per SNO event is set at 1000, which has been examined among other choices of sample size to generate result of sufficiently good quality. Any SNO events without minimally 1000 pixels of homogeneity better than 4.5% are excluded. Once an SNO event meets the criteria, all 1000 pixels of the best homogeneity quality are used to compute population statistics representative of the SNO event. The average of all 1000 pixel-based ratios is the radiometric ratio of the event, and the STD is the error bar, or "precision", of the average radiometric ratio. The collection of all event-based ratios and the error bars forms the comparison time series.

E. Precision

Finally, the precision of SNO events can vary over a wide range, from as precise as ~0.3% to as imprecise as 10% or higher. The cutoff choice definitively affects the time series result in both the quantity of comparison outcomes and the quality of the time series. Since OLCI provides only about two years of data to date, one of the challenges is to generate the best time series possible without excessive removal of outcomes. This analysis settles on 2% precision for a reasonable time series result. In addition, a 5%-precision result is also presented to display the more general two-year pattern for the purpose of demonstrating consistency with the 2%-precision result.

IV. Result

All inter-RSB comparison time series are shown in Figs. 2−4 over a 10% scale. The comparison time series using the 2% precision threshold is shown in blue squares while those of 5% precision is shown in red triangles. The blue solid line represents the series mean of the 2% precision time series, and the blue dotted lines marks 1% above and below the mean of 2% precision time series. No additional data adjustment schemes are applied for the purpose of keeping result clear and unambiguous. This includes not applying any special filter to remove outliers or any smoothing scheme. The two-year trend line to each 2% precision time series, shown in cyan dashed line, is the key outcome that demonstrates nominally correct on-orbit radiometric calibration on the level of statistics, which for this study is about 0.5% to 1.0%. All 2% precision time series has an average precision of 1.3%.

The case of Oa12 versus M6 is not shown because detector saturation of M6 over SNO scenes prevents the comparison time series from being built. For all cases, the 5% result is consistent with the 2% result, and for many cases the 5% result clearly shows the two-year trend where the 2% result may not be adequate to trace out the fuller trend.

A. Bands Oa02, Oa03, Oa04 and Oa06

The four comparison time series for the short-wavelength bands in Fig. 1 – Oa02 versus M1, Oa03 versus M2, Oa04 versus M3, and Oa06 versus M6 – may contain long-term radiometric drift. Various studies have shown short-wavelength bands of SNPP VIIRS [8-11] and twin MODIS [21,22] to contain worsening and long-term radiometric drifts. A dedicated study on MODIS and VIIRS [17] has proven the drifting error to come from a physical effect in one of the onboard calibration components, so-called "the degradation non-uniformity effect" in solar diffuser, that is not captured by the standard on-orbit calibration operation and analysis. It is possible that OLCI, which follows a similar on-orbit calibration approach, faces a similar calibration error in its short-wavelength bands.

The comparison time series of Oa02 and Oa03 (Figs. 2a and 2b) show the two-year result to be almost flat, and the trend lines indicate the overall change to be no worse than 0.3%. A soft yearly modulation of about 1% variation top-to-down can be seen, and the occurrences of successful comparison events are nicely spread out over the years. Even considering the presence of radiometric drift of VIIRS short-wavelength bands that can impact comparison result, which is at the level of about 0.3% per year [19], the time series result does not provide conclusive evidence that OLCI short-wavelength bands are drifting.

For Oa04 versus M3 and Oa06 versus M4, (Figs. 2c and 2d), the two-year trend fit is close to the 1% level. However, this change is consistent with the variability of the time series. These two time series show greater yearly modulation, which is attributed to the greater asymmetric difference in their spectral coverage (Table 2), as well as more outliers that can be traced to scenes of greater variability such as those of cloud. The two-year result is susceptible to outliers having high statistical leverage, and therefore these two time series need longer time interval for better reliability.

The result of these four band-pairs is consistent with known facts – if OLCI short-wavelength bands (those under 600 nm) drifts radiometrically, then the drift is consistent with that of MODIS and VIIRS at the level of about 0.3% per year. The "nadir-only" intersensor comparison analysis can possibly

detect the presence of the drift after about four years if the overall change has reached close to 1%.

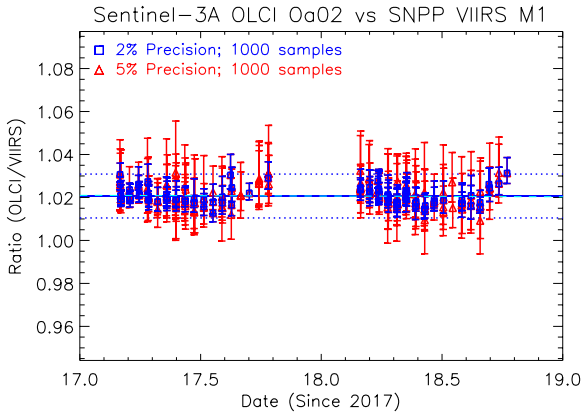

(a)

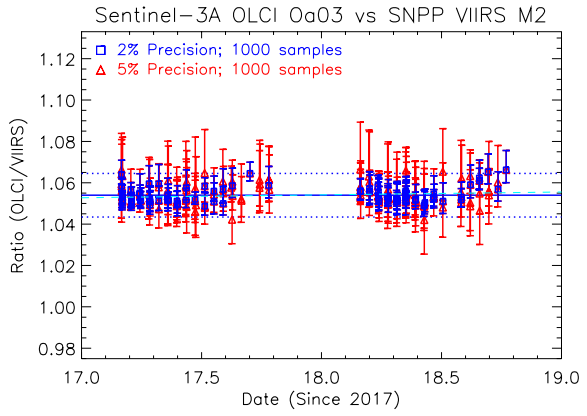

(b)

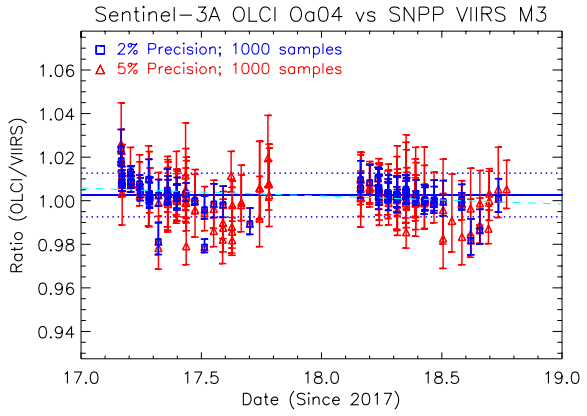

(c)

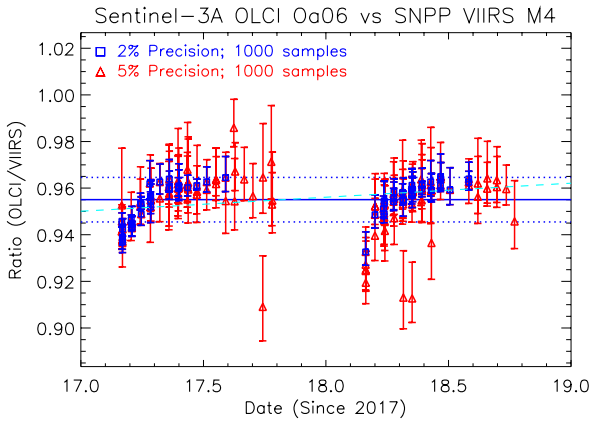

(d)

Figure 2: Two-year comparison time series for Sentinel-3A OLCI and SNPP VIIRS short wavelength bands for (a) Oa02 versus M1, (b) Oa03 versus M2, (c) Oa04 versus M3, and (d) Oa06 versus M4.

B. Bands Oa08, Oa09 and Oa10

The Oa08 versus M5 time series shows a stable two-year result, also consistent at the 0.3% level. Its yearly modulation is significantly weaker than previous band pairs and this is attributed to two key factors: spectral coverage being well matched and that bands of this wavelength are radiometrically more stable. Unlike M1 through M4, M5 is not known to have significant radiometric drift [17,18] and therefore this two-year 0.3% result can be interpreted as the expected statistical variation. This stable Oa08 result establishes the on-orbit OLCI calibration to be nominally correct in the middle wavelength range.

The three-band set of Oa08, Oa09 and Oa10 also provides an interesting case study to investigate the impact coming from the two sensors having some mismatch in their spectral coverage. Oa08, Oa09 and Oa10 are three spectrally adjacent bands overlapping with M5, thus each time series is the specific outcome due to the particular spectral response by each band to the same SNO scenes. Given all other conditions being identical, the different spectral coverage among three OLCI bands is the sole contributing factor to the different behavior in the time series.

The first notable, and expected, result is the different radiometric baselines (blue solid lines), at 1.007 for Oa08, 0.993 for Oa09, and 0.981 for Oa10, against M5. This is consistent with expectation, as the three bands will acquire different signal levels and generate different ratios against the signal of M5. The second notable, but not necessarily expected, is the different pattern of yearly modulation, with Oa08 showing very stable comparison result consistent with 1.007, and that Oa10 result shows the most variation from 0.995 to 0.970. The effect from the difference in the spectral coverage can mimic a seasonal pattern as the SNO scenes trace out different locations, hence different reflectance, over one year. Other differences such as different number of comparison events are also noticeable.

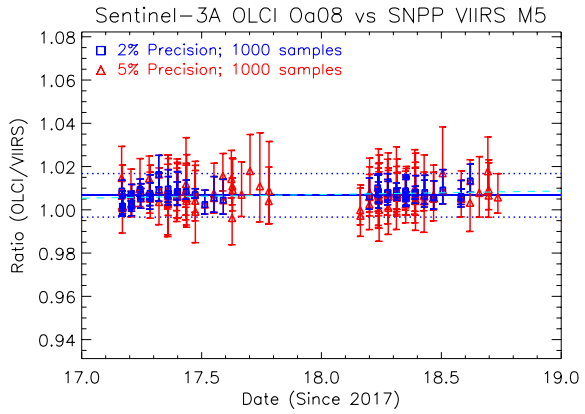

(a)

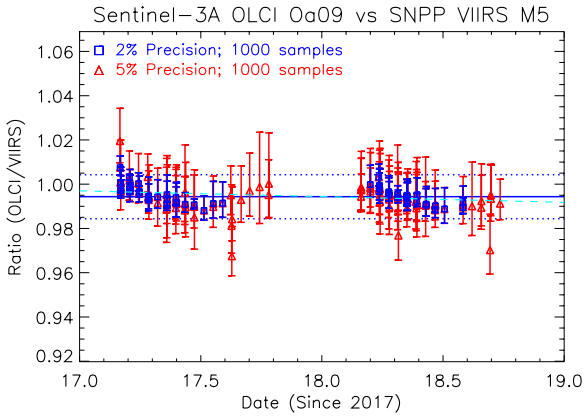

(b)

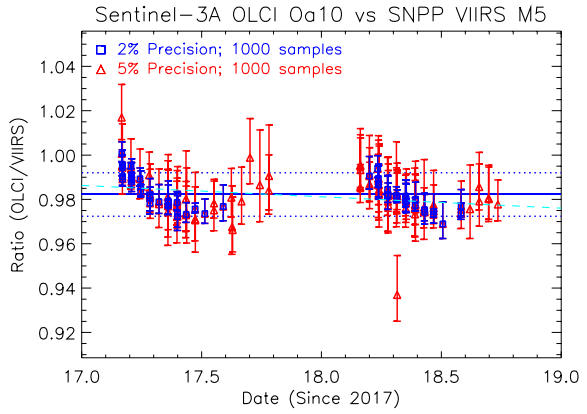

(c)

Figure 3: Two-year comparison time series for Sentinel-3A OLCI and SNPP VIIRS bands for (a) Oa08 versus M5, (b) Oa09 versus M5, and (c) Oa10 versus M5.

C. Band Oa17

Oa17 versus M7, in Fig. 4, is the final spectrally matching pair of OLCI and VIIRS (as per Table 2). This particular pair is also expected to generate a stable time series given their sufficiently good spectral match, the known stable behavior of the NIR bands, and the lack of any known serious calibration issues. One disadvantage of this pair is that the acquired signals at this wavelength over the SNO scenes are significantly weakened compared with those at shorter wavelength; hence fewer successful comparison outcomes are generated. Nevertheless, the 2% precision result can be seen to be stable at the level of –0.5% over two years, establishing the on-orbit calibration of OLCI to be nominally correct at the longer wavelength range. The 5%-precision time series is also consistent with the 2%-precision time series, thus further supports that Oa17 versus M7 is stable.

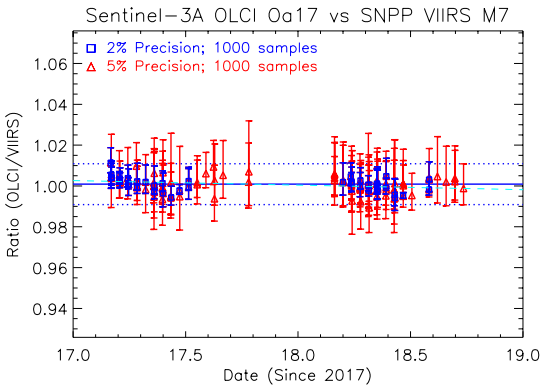

Figure 4. The two-year comparison time series for Sentinel-3A OLCI Oa17 versus SNPP VIIRS M7.

D. Summary Statistics

A summary statistics is given in Table 3 for those band-pairs with successful comparison result. The comparison baselines, the STD of the time series, and the two-year drift result are giving in column 5 through column 7. It can be seen that the comparison baselines vary over a wide range and do not necessarily reveal a clear relationship with respect to the degree of spectral mismatch. It is pointed out that a strong modulation effect, such as those in Oa04 and Oa06, makes very ambiguous the meaning of a radiometric baseline. In this regard, the time series STD and the two-year drift are particularly emphasized to support those cases where the result is less ambiguous. The cases for Oa02, Oa03, Oa08 and Oa17 are the four cases with stable yearly modulation pattern at the level of 0.3%, and therefore their two-year drift at the level of 0.3% (bold in column 7) is deemed consistent as well as reliable. The result of these four bands shows a consistent calibration result over the spectral range of OLCI.

V. Discussion

The evaluation of many OLCI bands cannot be performed due to the lack of spectral counterpart in VIIRS, and therefore the full evaluation will require additional effort such as using stable Earth scenes for monitoring. Nevertheless, the result of this study shows, consistently within statistics, that any possible drift is no worse than about 0.3% in the past two years.

This OLCI study provides an illustrative case study for the impact of the spectral mismatch through Oa08, Oa09 and Oa10. It is seen that the yearly modulation is connected to the imperfect spectral match between two matching bands, and that the temporal variations necessarily arise from varying responses over different scene types (with different reflectance property and radiometric response). The yearly modulation is

a feature commonly seen in various radiometric comparison studies [18,25,26]; yet there has not been a reliable systematic study on the impact of spectral mismatch. While it seems reasonable for one to perceive the modulation pattern to be related to geometry or geolocation, this result using three adjacent bands of identical geolocational condition for each SNO event provides a direct proof that the modulation pattern is not related to geolocational conditions such as solar-zenith angle.

Moreover, the comparison result of this OLCI study does not stand alone, but provides additional crosschecks or validation of other studies. In numerous inter-RSB comparison studies of Aqua MODIS versus SNPP VIIRS [18,25,26], the cause for many peculiar features remains unclear. For example, various Aqua MODIS versus SNPP VIIRS comparison time series exhibit significant yearly modulating features, with Aqua MODIS Band 1 (B1) versus SNPP VIIRS M5 having the most dramatic yearly variation minimally at 5% peak-to-trough [18]. Since intersensor comparison is relative, the comparison result requires additional input to determine which sensor is responsible for any particular features. In the case of M5, the result of this OLCI study further supports M5 (Fig. 3) to be stable at least on a short yearly term, and therefore the earlier Chu et al. [18] inter-RSB comparison study showing significant yearly modulation in Aqua MODIS B1 versus SNPP VIIRS M5 points to some additional effect in Aqua MODIS B1. In fact, similar argument can be made for the short-term stability of M1 and M2, leading to the possibility that other Aqua MODIS bands also have some peculiarity resulting in the strong variational pattern seen in the inter-RSB comparison of Aqua MODIS and SNPP VIIRS.

VI. Summary and Conclusion

The on-orbit calibration performance of Sentinel-3A OLCI is evaluated via a "nadir-only" intersensor comparison referencing to SNPP VIIRS. The time series of OLCI bands Oa02, Oa03, Oa08 and Oa17 demonstrate two-year radiometric stability on the level of ~0.3%. While short-wavelength OLCI bands may contain long-term radiometric drift as was found for MODIS and SNPP VIIRS, this two-year result shows any such possible drift to be below current statistics of about 0.3%. What can be stated is that the on-orbit RSB calibration for OLCI is nominally correct, meaning that the standard operational procedure and calibration analysis have performed as expected. It remains to be seen if effects such as the solar diffuser degradation non-uniformity can emerge at a later time. The "nadir-only" implementation of SNO approach, previously constructed for Aqua MODIS versus SNPP VIIRS, is also shown to be applicable to other pairs of sensors. With the coming era having more high performance multispectral sensors, a reliable intersensor comparison methodology with good precision capability will be highly beneficial. Lastly, this effort establishes a reasonable consistency between the VIS/NIR bands of Sentinel-3A OLCI and SNPP VIIRS, which is particularly important for the ocean color products.

Acknowledgment

This work was supported by the Joint Polar Satellite System (JPSS) funding. The views, opinions, and findings contained in this paper are those of the authors and should not be construed as an official NOAA or U.S. Government position, policy, or decision.

References

[1] C. Donlon, B. Berruti, A. Buongiorno, M.-H. Ferreira, P. Féménias, J. Frerick, P. Goryl, U. Klein, H. Laur, C. Mavrocordatos, J. Nieke, H. Rebhan, B. Seitz, J. Stroede, R. Sciarra, "The global monitoring for environment and security (GMES) sentinel-3 mission," Remote Sensing of Environment 120, 37-57 (2012).

[2] Sentinel-3 site; https://sentinel.esa.int/web/sentinel/missions/sentinel-3

[3] C. Cao, F. Deluccia, X. Xiong, R. Wolfe, F. Weng, "Early on-orbit performance of the Visible Infrared Imaging Radiometer Suite (VIIRS) onboard the Suomi National Polar-orbiting Partnership (S-NPP) satellite," IEEE Trans. Geosci. Remote Sens. 52, 1142–1156 (2014).

[4] A. K. Heidinger, C. Cao. and J. T. Sullivan, "Using Moderate Resolution Imaging Spectrometer (MODIS) to calibrate Advanced Very High Resolution Radiometer reflectance channels", *J. Geophys. Res.*, **107**, 4702 (2002).

[5] C. Cao and A. K. Heidinger, "Inter-comparison of the long-wave infrared channels of MODIS and AVHRR/NOAA-16 using simultaneous nadir observations at orbit intersections", *Earth Observing Systems VII (Proc. Of SPIE)*, **4814**, 306-316 (2002).

[6] C. Cao, M. Weinreb and H. Xu, "Predicting simultaneous nadir overpasses among polar-orbiting meteorological satellites for the intersatellite calibration of radiometers", *J. Atmos. Oceanic Technol.*, **21**, 537–542 (2004).

[7] J. Sun and M. Wang, "On-orbit characterization of the VIIRS solar diffuser and solar diffuser screen," Appl. Opt. 54, 236-252 (2015).

[8] J. Sun and M. Wang, "On-orbit calibration of the Visible Infrared Imaging Radiometer Suite reflective solar bands and its challenges using a solar diffuser," Appl. Opt. 54, 7210-7223 (2015).

[9] J. Sun and M. Wang, "Visible Infrared imaging radiometer suite solar diffuser calibration and its challenges using solar diffuser stability monitor", Appl. Opt. 53, 8571-8584 (2014).

[10] J. Sun and M. Wang, "Radiometric calibration of the visible infrared imaging radiometer suite reflective solar bands with robust characterizations and hybrid calibration coefficients," Appl. Opt., 54, 9331-9342 (2015).

[11] Wang, M., X. Liu, L. Jiang, S. Son, J. Sun, W. Shi, L. Tan, P. Naik, K. Mikelsons, X. Wang, and V. Lance, "VIIRS ocean color research and applications", Proc. IGARSS '15, pp.2911-2914 (2015).

[12] J. Sun and M. Wang, "VIIRS reflective solar bands calibration progress and its impact on ocean color products", Remote Sens. 8, 194 (2016).

[13] Wang, M., L. Jiang, X. Liu, S. Son, J. Sun, W. Shi, L. Tan, K. Mikelsons, X. Wang, and V. Lance, "VIIRS ocean color products: A progress update", Proc. IGARSS '16, pp.5848-5851 (2016).

[14] *NOAA Comprehensive Large Array-Data Stewardship System (CLASS)*. Accessed: March, 2019. [Online]. Available: https://www.bou.class.noaa.gov.

[15] J. Sun and M. Wang, "Reflective solar bands calibration improvements and look up tables for SNPP VIIRS operational mission-long SD reprocessing" Proc. SPIE 10402, Earth Observing Systems XXII, 104021W (2017)

[16] T. Choi, J. Sun, B. Zhang, Z. Wang, C. Cao, F. Weng, M. Wang, "Suomi-NPP initial reprocessing improvements and validations in the reflective solar bands (RSBs)", Proc. SPIE 10402, Earth Observing Systems XXII, 104021V (2017).

[17] J. Sun, M. Chu and M. Wang, "Degradation nonuniformity in the solar diffuser bidirectional reflectance distribution function," Appl. Opt. 55, 6001-6016 (2016).

[18] M. Chu, J. Sun and M. Wang, "Radiometric evaluation of the SNPP VIIRS reflective solar band sensor data records via inter-sensor comparison with Aqua MODIS", Proc. SPIE 9972, Earth Observing System XXI, 99721R (2016).

[19] M. Chu, J. Sun and M. Wang, "Performance evaluation of on-orbit calibration of SNPP VIIRS reflective solar bands via intersensor com- parison with *Aqua* MODIS," *J. Atmos. Ocean. Technol.*, vol. 35, no. 2, 385–403, 2018.

[20] M. Chu, J. Sun and M. Wang, "Radiometric Evaluation of SNPP VIIRS Band M11 via Sub-Kilometer Intercomparison with Aqua MODIS Band 7 over Snowy Scenes", *Remote Sens.*, 10, 413, (2018).

[21] J. Sun, X. Xiong, A. Angal, H. Chen, A. Wu, and X. Geng, "Time dependent response versus scan angle for MODIS reflective solar bands," *IEEE Trans. Geosci. Remote Sens.*, 52, 3159-3174 (2014).

[22] J. Sun, A. Angal, X. Xiong, H. Chen, X. Geng, A. Wu, T. Choi, and M. Chu, "MODIS RSB calibration improvements in Collection 6", Proc. SPIE 8528, 85280N (2012).

[24] Copernicus Open Access Hub: https://scihub.copernicus.eu/dhus/#/home.

[25] A. Wu, X. Xiong, C. Cao, and K. Chiang, "Assessment of SNPP VIIRS VIS/NIR radiometric calibration stability using Aqua MODIS and invariant surface targets," *IEEE Trans. Geosci. Remote Sens.*, **54,** (2016).

[26] S. Uprety, C. Cao, X. Xiong, S. Blonski, A. Wu, and X. Shao, "Radiometric intercomparison between Suomi-NPP VIIRS and Aqua MODIS reflective solar bands using simultaneous nadir overpass in the low latitudes," *J. Atmos. Ocean. Technol.*, **30**, 2720–2736(2013).

Table 1: Specifications and parameters for Sentinel-3A and SNPP satellites, OLCI and VIIRS.

	Sentinel-3A: OLCI	SNPP: VIIRS
Satellite Repeat Cycles (Days)	27	16
Satellite Local Crossing Time	Descending: 10:00 am	Ascending: 1:30 pm
Satellite Altitude (km)	814	834
Satellite Orbit Inclination	98.6	98.7
Sensor: Swath (km)	1270	3040
Sensor: Resolution at SSP (m)	300 m	750 m, 375 m
Sensor: Number of RSB/TEB/DNB	21/0/0	14/7/1

Table 2: The corresponding VIS/NIR bands of Sentinel-3A OLCI and SNPP VIIRS

Type	OLCI Band	Spectral Range (nm)	Spatial Resolution (m)	Lmax	VIIRS Band	Spectral Range (nm)	Spatial Resolution (m)	Lmax
VIS	**Oa02**	407–417	300	501.3	**M1**	402–422	750	135/615
	Oa03	438–448	300	466.1	**M2**	436–454	750	127/687
	Oa04	485–495	300	483.3	**M3**	478–498	750	107/702
	Oa06	555–565	300	524.5	**M4**	545–565	750	78/667
	Oa08/ (Oa09)/ (Oa10)	660–670/ (670–677.5)/ (677.5–685)	300	364.9/ (443.1)/ (350.3)	**M5**	662–682	750	59/651
					I1	600–680	375	718
NIR	**Oa12**	750–757.5	300	377.7	**M6**	739–754	750	41
	Oa17	856–876	300	229.5	**M7**	846–885	750	29/349
					I2	846–885	375	349
SWIR	(N/A)				**M8**	1230–1250	750	165

Table 3: Result of comparison baseline, time series standard deviation (STD) and the trend for the two-year drift.

OLCI Band	Spectral Range (nm)	VIIRS Band	Spectral Range (nm)	Comparison Baseline	Time Series STD (%)	2-Year Drift (%)
Oa02	407–417	**M1**	402–422	1.021	0.4	**-0.07**
Oa03	438–448	**M2**	436–454	1.054	0.4	**0.30**
Oa04	485–495	**M3**	478–498	1.002	0.7	-0.70
Oa06	555–565	**M4**	545–565	0.955	0.8	1.20
Oa08	660–670	**M5**	662–682	1.007	0.3	**0.30**
Oa09	670–677.5			0.995	0.4	-0.50
Oa10	677.5–685			0.982	0.7	-1.00
Oa17	856–876	**M7**	846–885	1.001	0.3	**-0.50**